NeuroImage: Clinical 35 (2022) 103127

Contents lists available at ScienceDirect

NeuroImage: Clinical

journal homepage: www.elsevier.com/locate/ynicl

Functional connectivity in the dorsal network of the cervical spinal cord is correlated with diffusion tensor imaging indices in relapsing-remitting multiple sclerosis

Anna J.E. Combes [a,b,*], Kristin P. O'Grady [a,b], Baxter P. Rogers [a,b], Kurt G. Schilling [a,b], Richard D. Lawless [a,c], Mereze Visagie [a], Delaney Houston [a], Logan Prock [a], Shekinah Malone [d], Sanjana Satish [a], Atlee A. Witt [a], Colin D. McKnight [b], Francesca Bagnato [e,f], John C. Gore [a,b,c], Seth A. Smith [a,b,c]

[a] Vanderbilt University Institute of Imaging Science, Vanderbilt University Medical Center, 1161 21st Avenue South, Medical Center North, AA-1105, Nashville, TN 37232-2310, United States
[b] Department of Radiology and Radiological Sciences, Vanderbilt University Medical Center, Medical Center North, 1161 21st Ave. South, Nashville, TN 37232, United States
[c] Department of Biomedical Engineering, Vanderbilt University, 2301 Vanderbilt Place, PMB 351826, Nashville, TN 37235-1826, United States
[d] School of Medicine, Meharry Medical College, 1005 Dr. D. B. Todd, Jr. Blvd., Nashville, TN 37208, United States
[e] Neuroimaging Unit, Neuroimmunology Division, Department of Neurology, Vanderbilt University Medical Center, 1161 21st Ave. South, A-0118 Medical Center North, Nashville, TN 37232, United States
[f] Department of Neurology, Nashville VA Medical Center, TN Valley Healthcare System, 1310 24th Avenue South, Nashville, TN 37212-2637, United States

ARTICLE INFO

Keywords:
Spinal cord
Multiple sclerosis
Resting-state fMRI
Functional connectivity
Diffusion tensor imaging

ABSTRACT

Focal lesions may affect functional connectivity (FC) of the ventral and dorsal networks in the cervical spinal cord of people with relapsing-remitting multiple sclerosis (RRMS). Resting-state FC can be measured using functional MRI (fMRI) at 3T. This study sought to determine whether alterations in FC may be related to the degree of damage in the normal-appearing tissue. Tissue integrity and FC in the cervical spinal cord were assessed with diffusion tensor imaging (DTI) and resting-state fMRI, respectively, in a group of 26 RRMS participants with high cervical lesion load, low disability, and minimally impaired sensorimotor function, and healthy controls. Lower fractional anisotropy (FA) and higher radial diffusivity (RD) were observed in the normal-appearing white matter in the RRMS group relative to controls. Average FC in ventral and dorsal networks was similar between groups. Significant associations were found between higher FC in the dorsal sensory network and several DTI markers of pathology in the normal-appearing tissue. In the normal-appearing grey matter, dorsal FC was positively correlated with axial diffusivity (AD) ($r = 0.46$, $p = 0.020$) and mean diffusivity (MD) ($r = 0.43$, $p = 0.032$). In the normal-appearing white matter, dorsal FC was negatively correlated with FA ($r = -0.43$, $p = 0.028$) and positively correlated with RD ($r = 0.49$, $p = 0.012$), AD ($r = 0.42$, $p = 0.037$) and MD ($r = 0.53$, $p = 0.006$). These results suggest that increased connectivity, while remaining within the normal range, may represent a compensatory mechanism in response to structural damage in support of preserved sensory function in RRMS.

1. Introduction

Cervical spinal cord (CSC) pathology is an important cause of disability for people with relapsing-remitting multiple sclerosis (RRMS). Advanced quantitative magnetic resonance imaging (MRI) measures of cord tissue integrity and function have the potential to provide information on pathology beyond atrophy and lesion burden, two routinely-used markers that each come with limitations in representing disease progression and explaining clinical impairment. Further characterization of tissue injury in the CSC, which encompasses both focal lesions and microscopic changes in the normal-appearing tissue, can be obtained with diffusion tensor imaging (DTI). DTI indices in the spinal

* Corresponding author at: 1161 21st Avenue South, MCN AA1105, Nashville, TN 37232, United States.
E-mail address: anna.combes@vumc.org (A.J.E. Combes).

https://doi.org/10.1016/j.nicl.2022.103127
Received 11 January 2022; Received in revised form 3 June 2022; Accepted 23 July 2022
Available online 27 July 2022

cord have been shown to be sensitive to demyelination in both lesioned and normal-appearing tissue (Klawiter et al., 2011) and have demonstrated correlations with disability (Ciccarelli et al., 2007; Kearney et al., 2015; Naismith et al., 2013).

Beyond structural damage, widespread alterations in neuronal activation probed with functional MRI (fMRI) have been observed in the brain of people with RRMS. Increases in functional connectivity (FC), shown using resting-state fMRI (rs-fMRI), were found to be associated with cognitive impairment (Cader et al., 2006; Hawellek et al., 2011) and overall disability (Faivre et al., 2016), particularly in the sensorimotor network (Strik et al., 2021). Task-based fMRI studies in the CSC have shown increased activation and overall altered recruitment patterns in response to tactile stimuli in RRMS (Agosta et al., 2008a; Agosta et al., 2008b; Valsasina et al., 2012), with more pronounced effects in patients with more severe disability (Valsasina et al., 2010). One study also found a link between extent of recruitment during tactile stimulation and fatigue (Rocca et al., 2012). Potentially, therefore, resting-state patterns of neuronal activity in the cord may also be altered. The only previous resting-state study of the cord in MS, performed at 7T, found no global differences in FC between MS participants and controls, but observed complex effects of lesion location, column-wise and in the rostro-caudal axis, on different seed-based connectivity metrics in within-segment networks (Conrad et al., 2018). The impact of MS pathology on CSC resting-state connectivity beyond those observations remains largely unknown, and the relationship between FC and tissue damage beyond focal lesions has not yet been assessed. Investigating this phenomenon is relevant to clinicians, as it would aid understand the potential impact of lesions on clinically hidden functional changes, the exhaustion of which eventually leads to irreversible disability. Such an assessment is also particularly important in patients with low disability, as they are those for whom strategies can still be implemented to prevent neurological decline, should a target for intervention be identified.

Thus, we sought to determine whether: (1) FC abnormalities could be detected in minimally disabled participants with evidence of tissue damage beyond lesions; (2) FC was also related to the degree of non-lesional tissue damage; and (3) FC was related to sensorimotor clinical function.

2. Materials and methods

2.1. Data acquisition

Twenty-eight participants with RRMS (Thompson et al., 2018) and 25 sex- and age-matched healthy controls (HC) were consecutively and prospectively enrolled. Inclusion criteria for patients included an Expanded Disability Status Scale (Kurtzke, 1983) (EDSS) score ≤ 2, and known CSC involvement based on the presence of cervical lesions on the most recent clinical MRI. Two RRMS participants were excluded upon visual inspection of the data (39-year-old female, heavy distortions in the DTI data; 42-year-old female, poor fMRI quality owing to presence of metal in clothing). The final sample consisted in 26 participants with RRMS and 25 healthy controls (Table 1). All studies were approved by the local institutional review board and signed informed consent was obtained prior to participation.

Participants completed a sensorimotor exam including the Timed Up and Go test (Nilsagard et al., 2007) (TUG) and lower extremity vibration threshold measurements using a Vibratron-II device (Newsome et al., 2011). The average time of two TUG trials was calculated. Vibration testing was performed bilaterally on the big toe using a descending method of limits, and the average right and left thresholds were averaged.

On the same study day, participants were scanned on a 3T Philips Elition (Philips Medical Systems, Best, The Netherlands) using a 16-channel neurovascular coil for reception and a 2-channel body coil for signal transmission. Physiological data were acquired using chest bellows and a peripheral pulse oximeter with a sampling rate of 496 Hertz (Hz). Images were centered at the C3/C4 disk space and covered the same superior-inferior field of view. The acquisition protocol included the following sequences.

Table 1
Demographic and clinical measures for the control and MS groups.

	Healthy Controls (n = 25)	Multiple Sclerosis (n = 26)	p-value
Sex at birth	14F/11 M	16F/10 M	NS
Age (years)[a]	28.9 ± 6.1	31.8 ± 6.1	NS
Years of disease[b]	–	2.6 (0.1–20.0)	–
EDSS[b]	–	0.5 (0–2)	–
TUG (seconds)[a]	6.10 ± 1.06	7.30 ± 1.87	**0.008****
Vibration threshold[a]	1.29 ± 0.49	1.81 ± 1.31	0.07

Sensorimotor data were not available for one control participant (28-year-old male). All comparisons performed with Student's t-tests, except sex at birth with a chi-square test.
EDSS = Expanded Disability Status Scale score; NS = non-significant; TUG = Timed Up and Go. Significant at **$p < 0.01$. [a]Indicates mean ± standard deviation; [b]indicates median (range).

- Sagittal T2-weighted turbo spin echo, TR/TE = 2500/100 ms, $\alpha = 90°$, FOV = 160 × 250 mm^2, 18 slices, voxel size 0.8 × 1 × 2mm^3 (reconstructed to 0.49 × 0.49 × 2mm^3).
- PD/T2*-weighted axial anatomical scan: multi-echo Fast Field Echo (mFFE), TR/TE = 700/8ms, $\alpha = 28°$, FOV = 160 × 160 mm^2, 14 slices, voxel size 0.65 × 0.65 × 5mm^3 (reconstructed to 0.31 × 0.31 × 5mm^3).
- Resting-state functional run: 3D axial multishot gradient echo, volume acquisition time = 2.46 s, TE = 20 ms, $\alpha = 8°$, FOV = 150 × 150mm^2, 14 slices, voxel size 1 × 1 × 10mm^3 (reconstructed to 0.59 × 0.59 × 5mm^3), 200 dynamics (~8 min), EPI factor = 9.
- Cardiac-triggered, single-shot EPI diffusion sequence: TR = 5 beats (~4000 ms), TE = 77 ms, SENSE (RL) = 1.8, FOV = 80 × 57.5 × 70mm^3, 14 slices, resolution = 1.1 × 1.1 × 5mm^3, averages = 3. A single-shell acquisition was used with 15 directions at b = 750 s/mm^2.

2.2. Image processing

All processing steps were performed using FSL v6.0.4 (Smith et al., 2004) and Spinal Cord Toolbox (SCT) v4.0.2 (De Leener et al., 2017) unless specified otherwise.

2.2.1. Anatomical preprocessing

Cord segmentations were obtained on the sagittal T2 and axial mFFE scans using *sct_deepseg_sc*, and both images were co-registered. Vertebral levels were automatically identified on the sagittal T2 using SCT and transformed into mFFE space. In order to include anatomically consistent regions between participants, only slices corresponding to the C3 and C4 vertebral levels were retained for further analysis. Grey matter (GM) masks were obtained on the mFFE image using *sct_deepseg_gm*, and manually corrected where necessary. In the presence of lesions obscuring GM/WM boundaries, the 'butterfly' shape provided by the segmentation model was used as a starting point, and information on GM contour gained from adjacent slices. WM masks were obtained by subtracting the GM from the cord mask. Slicewise cross-sectional area (CSA) and GM CSA, corrected for cord angle, were obtained and averaged within slices at the C3 and C4 vertebral levels. Lesion masks were drawn manually on the MS participants' mFFE images by an experienced neuroradiologist (CMK) using ITK-SNAP. Lesion fraction within the volume of interest was calculated for GM and WM as the proportion of voxels within the lesion mask to the respective tissue masks.

2.2.2. fMRI processing

fMRI preprocessing was conducted using SCT and in-house code implemented in Matlab R2018b and Python 3.6.9. First, data were motion-corrected, including the extraction of x- and y-plane motion parameters. *sct_deepseg_sc* was used on the resulting mean functional image to obtain cord and CSF masks, which were manually edited where necessary. Whole-slice masks were obtained by subtracting the dilated cord and CSF masks from the whole image. Physiological signals corresponding to the respiratory cycle and cardiac rhythm were calculated using AFNI-RETROICOR (Glover et al., 2000). Structured noise signals within the global and CSF masks were identified slicewise using principal component analysis, as described in Barry et al. (Barry et al., 2016). The obtained physiological, CSF and global signal, and motion correction parameters were regressed out from the functional run at each voxel. The denoised time-series were then band-pass filtered with a Chebyshev Type II filter using cutoffs of 0.01 and 0.10 Hz.

GM regions of interest (ROIs) were created by segmenting GM on the anatomical mFFE and registering both images to functional space, partitioning the resulting mask into quadrants, and discarding the central GM commissure. To ensure adequate ROI selection, slices were retained only when GM ROIs were $\geq$ 4 voxels in the reconstructed resolution ($\sim$1.7 mm^3); this was based on practical experience obtaining robust segmentations. Average time-series were obtained for each GM horn. Pearson correlation coefficients and corresponding Fisher z-scores, correcting for first-order autocorrelation as described by Rogers et al. (2008), were computed for each slice between the ventral, and the dorsal GM horns. Median ventral and dorsal network FC z-scores (subsequently referred to as ventral and dorsal z-scores) for each subject were calculated across slices at the C3 and C4 levels concurrently. The temporal signal-to-noise ratio (tSNR) was calculated voxelwise, after nuisance regression and before band-pass filtering, as the ratio of the mean signal over time over the standard deviation of the time-series. The voxelwise tSNR values were then averaged within the GM to obtain one value per subject.

2.2.3. DTI processing

Diffusion data were motion-corrected, and model fitting was performed with SCT to obtain fractional anisotropy (FA), radial (RD), axial (AD), and mean diffusivity (MD) maps. The mean motion-corrected diffusion-weighted image was segmented to obtain a cord mask in diffusion space, and the mFFE and corresponding GM, WM, lesion, and vertebral levels masks were transformed into diffusion space using a nonlinear warp to account for distortions in diffusion-weighted images. Mean values for normal-appearing GM (NAGM), WM (NAWM), and lesioned tissue were calculated across slices corresponding to the C3 and C4 vertebral levels.

2.3. Statistical analysis

Statistical analyses were carried out in R v3.6.3 (R Core Team, 2017). Demographic, morphometric, DTI indices (FA, RD, AD and MD) in the normal-appearing and lesioned GM and WM, and FC indices (ventral and dorsal network z-scores) were compared between groups using Student's *t*-test. Ventral and dorsal z-scores, and normal-appearing and lesioned tissue DTI metrics within the MS group, were compared within-subject using paired t-tests. In each group, correlations between DTI and FC metrics were computed using Pearson's correlation coefficient. Further, we conducted partial correlation analyses to assess the relationship between DTI-derived indices and z-scores with age, disease duration, GM and WM lesion fraction, and tSNR of the functional acquisition as covariates of no interest. Finally, the relationships between connectivity z-scores and EDSS, TUG, and vibration threshold, and between DTI indices and EDSS were tested using Spearman's rank correlation coefficient. In addition to significant findings ($\alpha = 0.05$), we report results at the trend level ($p < 0.10$) due to the exploratory nature of this study.

3. Results

3.1. Group comparisons

Demographic details and sensorimotor results are reported in Table 1. Participants with MS had significantly longer TUG times than controls ($p = 0.008$) but showed no difference on the vibration threshold test (although a trend was observed, $p = 0.07$). Example images, segmented regions of interest and quantitative DTI-derived maps for one control and one participant with MS are shown in Fig. 1. Representative functional data for one subject can be found in Supplemental Fig. 1. The obtained morphometric, fMRI and DTI-derived indices and group comparisons are reported in Table 2.

Cord and GM CSA did not differ between the groups. The median lesion fraction in MS participants was 5% in the GM and 13% in the WM. All patients had WM lesions, and all but four had lesions in the GM.

Exclusion of small GM horn regions (<4 voxels) resulted in the dorsal network z-score for one MS participant (23-year-old female) being discarded. For both groups, the average ventral z-score was higher than the dorsal z-score (both $p < 0.0001$). Ventral and dorsal z-scores did not differ between HC and MS (Fig. 2**A**). There was no significant difference in tSNR between groups.

Group comparisons of DTI metrics are shown in Fig. 3. There were no significant group differences in NAGM. GM lesions differed from control values for FA ($p = 0.044$) and RD ($p = 0.019$), and at the trend level for MD ($p = 0.07$). In the NAWM, FA was significantly lower ($p = 0.009$) and RD significantly higher ($p = 0.032$) in the MS group compared to controls. In WM lesions, FA was lower ($p = 0.002$), and both RD ($p = 0.002$) and MD ($p = 0.001$) were higher in the MS group compared to healthy WM. Comparisons between lesioned and NA tissue in the MS group are reported in Table 2.

3.2. Correlations between DTI and fMRI

There were no significant correlations between DTI and FC indices in the control group, except for dorsal z-score which showed trends with FA ($r = -0.37$, $p = 0.065$) and RD ($r = 0.35$, $p = 0.089$) in the WM (data not shown). In the MS group, ventral network z-scores were not related to any of the DTI parameters (Supplemental Fig. 2).

Several correlations were observed between dorsal z-scores and DTI indices in the MS group (Fig. 4). In the NAGM, dorsal z-scores were positively correlated with AD ($r = 0.46$, $p = 0.020$) and MD ($r = 0.43$, $p = 0.032$). In the NAWM, dorsal z-scores were correlated with all DTI indices: lower FA ($r = -0.43$, $p = 0.028$), and higher RD ($r = 0.49$, $p = 0.012$), AD ($r = 0.42$, $p = 0.037$) and MD ($r = 0.53$, $p = 0.006$).

Additional analyses evaluated the potential confounding effects of covariates (age, disease duration, GM and WM lesion fraction, and tSNR of the functional run) on the observed correlations. Of the six significant correlations above detailed, all remained significant after the addition of the covariates above (data not shown) except that seen between dorsal z-score and mean FA in the NAWM ($r = -0.39$, $p = 0.092$).

3.3. Associations with clinical measures in MS

The distribution of z-scores by EDSS within the MS group is shown in Fig. 2**B**. There was no significant relationship between EDSS and either ventral or dorsal z-scores ($p > 0.05$). Regarding DTI metrics, decreased FA in the NAWM was significantly associated with higher EDSS scores ($rho = -0.42$, $p = 0.034$), and RD showed a trend in the opposite direction ($rho = 0.38$, $p = 0.051$) (Supplemental Fig. 3). TUG and vibration threshold were not correlated with z-scores (Supplemental Fig. 4).

4. Discussion

We used DTI and rs-fMRI to compare indices of structural integrity and FC in the CSC of participants with RRMS with low disability (EDSS

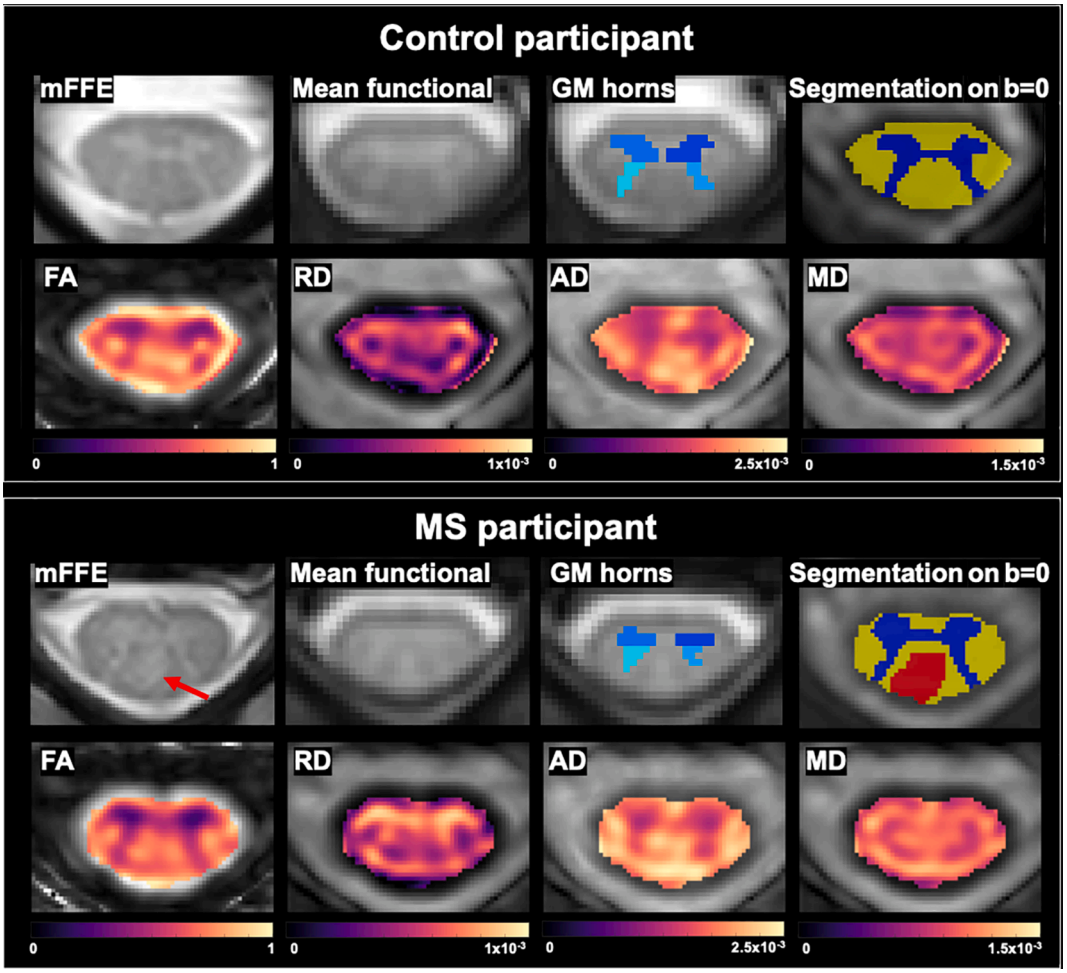

Fig. 1. Example data for one control (25-year-old female) and one participant with MS (25-year-old female, EDSS 0, disease duration < 1 year). Shown are the mFFE anatomical image used for lesion identification, vertebral level identification and segmentation; the average functional image showing grey/white matter contrast after motion correction; grey matter horns regions of interest in functional space used to derive functional correlations; tissue type segmentations in diffusion space overlaid on a b = 0 image; and FA, RD, AD and MD quantitative maps. A dorsal column lesion in the MS participant is shown with a red arrow, and the corresponding lesion mask in DTI space in red on the segmentation image. (For interpretation of the references to colour in this figure legend, the reader is referred to the web version of this article.)

≤ 2) and controls. We found evidence of lesioned and normal-appearing tissue changes measured with DTI in both the GM and WM but overall preserved connectivity. RD and MD in the NAGM, and all indices in the NAWM indicative of tissue damage were significantly correlated with higher FC in the dorsal sensory network. These findings are discussed in further detail below.

4.1. Structural changes

Median CSC lesion fraction was 5% within GM and 13% within WM. While this is higher than previous reports (Eden et al., 2019), we specifically recruited patients with known CSC involvement on clinical scans, all with evident cord lesions. Moreover, lesion fraction was calculated within the C3 and C4 levels, the areas with the highest lesion frequency in the CSC (Eden et al., 2019). We observed no significant whole-cord atrophy in this sample of relatively young people with the RR subtype and low EDSS scores. While cord atrophy can be measured early in the disease course, including in clinically isolated syndrome (Casserly et al., 2018), this may not have been detectable with the current sample size. Moreover, focal lesions, which were highly prevalent in this group, can cause both swelling or volume loss, which may have competing effects on measured CSA (Biberacher et al., 2015). In the GM, CSA and DTI parameters were similar between MS and control participants, despite the high lesion load noted above. GM neuronal loss is not always detectable in RRMS patients with low disability (Chen et al., 2020), and may not yet be visible in this cohort. Additionally, the adequacy of DTI in probing GM damage is limited, and DTI measures have lower SNR in GM than WM. In the NAWM, FA and RD were significantly different from controls, indicating loss of fiber coherence and demyelination, respectively. This has been noted in several studies of RRMS (Cohen et al., 2017; Martin et al., 2016), and could be linked to the high prevalence of lesions in the imaged volumes, as damage is more commonly seen in regions adjacent to lesions (Moll et al., 2011; Vrenken et al., 2006), as well as microstructural damage (Van Hecke et al., 2009). FA in NAWM was also significantly correlated with EDSS score, with lower values found in patients with greater impairment (and a corresponding trend seen with increased RD). Finally, several DTI indices were different in both lesioned GM and WM, reflecting demyelination and axonal loss (Cohen et al., 2017; Sbardella et al., 2013). In both tissue types, reduced FA is linked with loss of myelin and expansion of the extracellular space (Sbardella et al., 2013), while increased RD reflects the severity of myelin injury and demyelination (Klawiter et al., 2011). The increase in MD in WM lesions (and at the trend level in GM lesions) can likely be attributed to the increase in RD. AD was significantly higher in WM lesions compared to NAWM. A possible explanation is that in WM lesions past the acute stage, elevated AD may reflect cellular

Table 2
Comparison of anatomical, diffusion tensor imaging, and functional indices between groups.

	HC (n = 25)	MS (n = 26)	p-value	
Morphometry				
CSA, mm^2	82.77 ± 10.18	81.20 ± 6.54	NS	
GM CSA, mm^2	17.01 ± 1.62	16.51 ± 1.24	NS	
Percent lesion fraction in GM[a]	–	5 (0–98)	–	
Percent lesion fraction in WM[a]	–	13 (0–75)	–	
Functional connectivity				
Ventral network (z-score)	7.14 ± 1.79	7.67 ± 1.92	NS	
Dorsal network (z-score)	4.80 ± 1.81	5.14 ± 1.73	NS	
tSNR	21.95 ± 4.33	19.63 ± 5.73	NS	
DTI indices in NAGM				
FA	0.588 ± 0.056	0.568 ± 0.051	NS	
RD, mm^2/s x10^{-4}	5.70 ± 0.74	6.00 ± 0.86	NS	
AD, mm^2/s x10^{-4}	16.13 ± 0.65	16.09 ± 0.97	NS	
MD, mm^2/s x10^{-4}	9.18 ± 0.45	9.37 ± 0.77	NS	
DTI indices in NAWM				
FA	0.753 ± 0.048	0.715 ± 0.052	**0.009****	
RD, mm^2/s x10^{-4}	4.23 ± 0.81	4.78 ± 0.95	**0.032***	
AD, mm^2/s x10^{-4}	19.23 ± 0.57	18.96 ± 0.75	NS	
MD, mm^2/s x10^{-4}	9.23 ± 0.53	9.51 ± 0.79	NS	
DTI indices in GM lesions			**vs HC group**	**vs MS group**
FA	–	0.548 ± 0.070	**0.044***	NS
RD, mm^2/s x10^{-4}	–	6.25 ± 0.76	**0.019***	NS
AD, mm^2/s x10^{-4}	–	16.09 ± 1.59	NS	NS
MD, mm^2/s x10^{-4}	–	9.53 ± 0.75	0.07	NS
DTI indices in WM lesions				
FA	–	0.701 ± 0.064	**0.002****	0.08
RD, mm^2/s x10^{-4}	–	5.12 ± 1.08	**0.002****	**0.006****
AD, mm^2/s x10^{-4}	–	19.55 ± 1.19	NS	**0.0004*****
MD, mm^2/s x10^{-4}	–	9.93 ± 0.87	**0.001****	**0.0001*****

All values are reported as mean ± standard deviation unless specified otherwise. Group comparisons were performed with Student's t-tests, and diffusion metrics in normal-appearing vs lesioned tissue in the multiple sclerosis group with paired t-tests. Dorsal network data were not available for one MS participant (23-year-old female) due to image quality.
AD = axial diffusivity; CSA = cross-sectional area; DTI = diffusion tensor imaging; FA = fractional anisotropy; GM = grey matter; HC = healthy controls; MD = mean diffusivity; NA = normal-appearing; NS = non-significant; RD = radial diffusivity; tSNR = temporal signal-to-noise ratio; WM = white matter. Significant at *p < 0.05, **p < 0.01, ***p < 0.001. [a]Indicates median (range).

responses to injury, such as gliosis and cellular infiltration (Aung et al., 2013).

4.2. Resting-state functional connectivity and associations with tissue damage

We found that ventral connectivity was higher than dorsal connectivity in both groups. This has been a consistent finding in some (Conrad et al., 2018; Kong et al., 2014), but not all (Eippert et al., 2017), studies of CSC connectivity so far.

We observed that FC in the RRMS group was similar to controls' in both networks. Preserved connectivity has previously been observed by Conrad et al. (2018) in 22 patients with RRMS. Such preservation may indicate the known ability of the central nervous system to compensate for tissue injury by maintaining adequate resting-state network activity. Here, dorsal FC was positively correlated with all indices of NAWM pathology, and specifically biologically relevant indices of NAGM damage. The interpretation of NAWM changes in FA and RD is discussed in the previous section. In both NAWM and NAGM, AD and MD were similar to the control group, but both were positively correlated with increased dorsal connectivity. In NA tissue, higher AD may reflect reparatory processes indicative of more long-standing damage (Aung et al., 2013) which would be found in those subjects with a compensatory increase in connectivity. Increased MD, while unspecific, is indicative of increased diffusivity and general loss of tissue integrity and likely reflects the accompanying changes in AD and RD. An earlier study of task-based fMRI in the RRMS cord showed significant associations between FA and MD values and increased signal change in response a proprioceptive stimulation (Agosta et al., 2008b). Conrad and colleagues (Conrad et al., 2018) found that in-slice lateral and dorsal WM lesions tended to increase dorsal FC, and hypothesized that increased FC would be found in the MS cord, based on the brain rs-fMRI and task-based spinal cord fMRI literature. Increased brain resting-state FC has been observed in RRMS, especially in the early stage of disease before the accumulation of structural damage and before exhaustion of efficient functional compensatory mechanisms (Basile et al., 2014; Faivre et al., 2016; Strik et al., 2021; Tommasin et al., 2018). We can therefore postulate that the higher FC observed in those patients with greater tissue damage may reflect an adaptive compensatory response in reaction to tissue injury in order to preserve clinical function. Those patients with preserved connectivity in the presence of lesions may represent the ideal candidate group for whom neuroprotective strategies maintaining 'healthy' network connectivity could be indicated and have maximal efficiency.

Two relationships at the trend level were observed in controls: higher dorsal z-score with lower WM FA and higher RD (both $p < 0.10$). All participants were under 42 years old, likely precluding age effects. A possible explanation may be a mediating effect of data quality (e.g. participant motion) that would concurrently affect DTI and FC measures. Others have warned on signal quality confounding group effects in rs-fMRI analysis, specifically in the context of MS (Baijot et al., 2021). However, the addition of tSNR as a covariate did not overall affect the correlations between DTI indices and dorsal connectivity. Other properties of the fMRI signal that may be specific to MS, such as intrinsic vascular and neuronal activity characteristics, could be further investigated with methods like analysis of the amplitude of low frequency fluctuations (Zang et al., 2007).

4.3. Limitations and future directions

Some methodological considerations should be discussed. First, the low-pass filter cut-off was set at 0.10 Hz. A previous investigation showed benefit in using a higher cut-off for detecting higher correlations

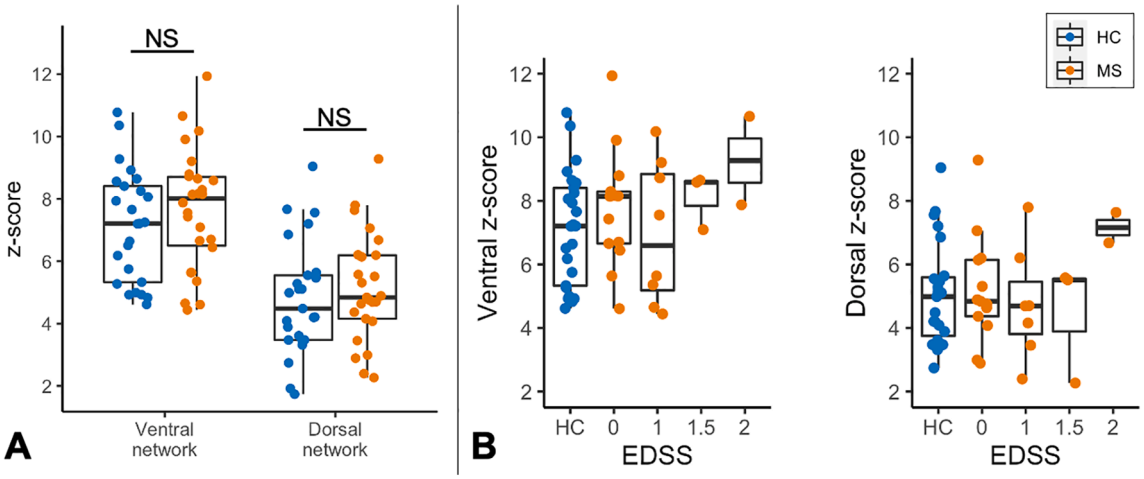

Fig. 2. **(A)** Functional connectivity indices between groups. Ventral and dorsal network z-scores do not significantly differ between control and MS participants. **(B)** Distribution of z-scores by EDSS in MS participants compared to controls' values. Note the EDSS scale is not continuous. One dorsal z-score is missing for one MS participant (23-year-old female) due to data quality.

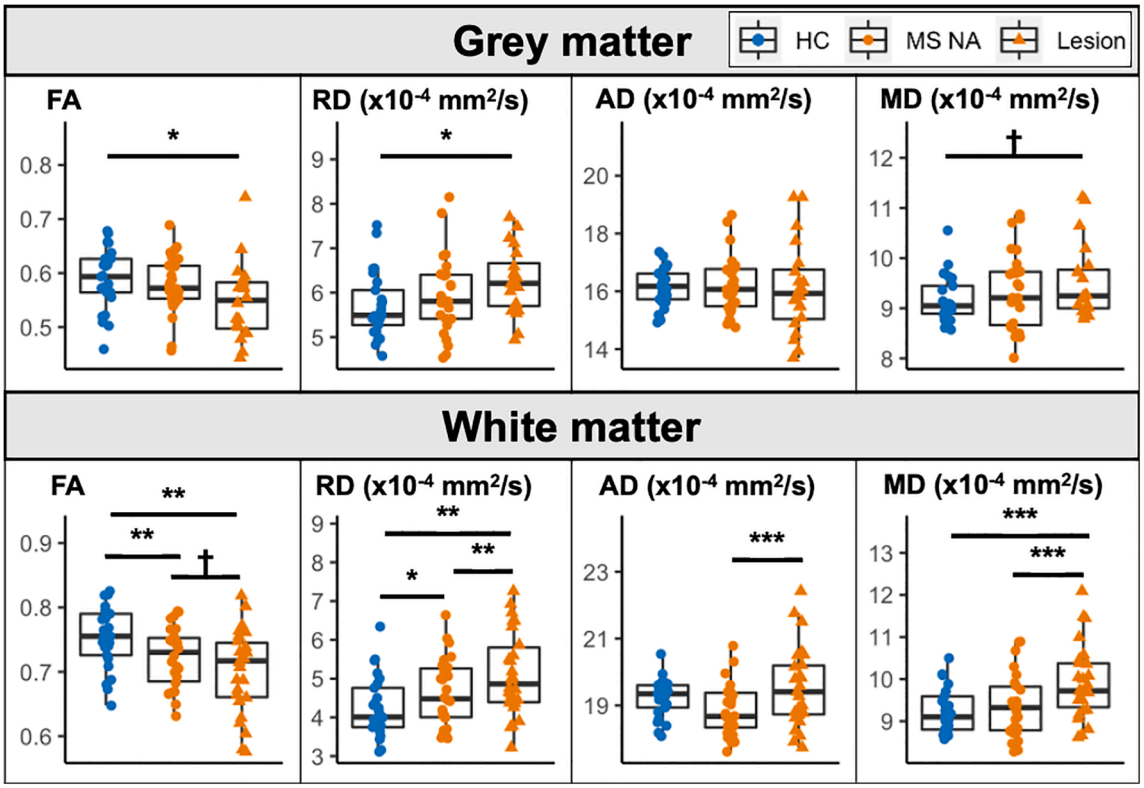

Fig. 3. Comparison of DTI values in GM and WM between controls, MS normal-appearing and lesioned tissue. †Trend level result ($p < 0.10$, non-significant). Significant at *$p < 0.05$, **$p < 0.01$, ***$p < 0.001$.

between regions (Barry et al., 2018). Our volume acquisition time of 2.46 s theoretically enables the detection of signals at frequencies up to 0.20 Hz. However, the characteristics of blood oxygen level-dependent fluctuations in the spinal cord have yet to be investigated in detail, and a more conservative 0.10 Hz cut-off as chosen here is used in most brain studies (Powers et al., 2018). Second, signal from the surrounding WM was not regressed out from the GM signal, as the relationships between possibly meaningful WM fluctuations and GM activation are not fully known (Mazerolle et al., 2013); this could have influenced the robustness of the obtained correlations (Brooks et al., 2017). Third, the MS group contained more female than male participants, which is representative of the demographic makeup of RRMS. One study suggested the possibility of higher FC in healthy female participants (Conrad et al., 2018). Though the proportion of female participants in each group was matched in this study, a larger sample size would help disentangle the effects of disease status, age, and sex. Fourth, a detailed analysis of the influence of lesion location such as that performed by Conrad et al. (2018) was outside the scope of this project. No differentiation was made between different WM tracts, and between metrics up- or downstream of lesions. Thus, there is variation in the neuroanatomical relationship between the GM neurons and the WM tracts that were assessed. Moreover, the up- and downstream effects of tissue damage to

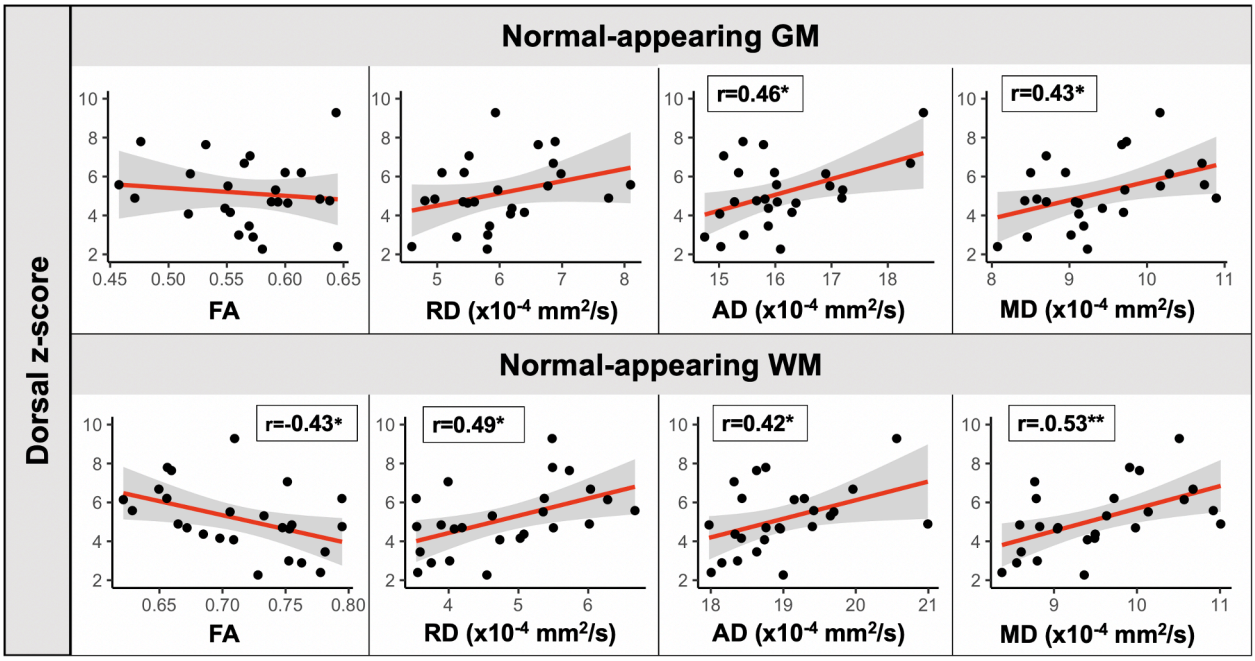

Fig. 4. Correlations between normal-appearing grey and white matter DTI indices and dorsal (sensory) z-scores in the MS group. Pearson's r correlation coefficients are reported. Line and shaded area represent linear regression line and 95% confidence intervals. Significant at *p < 0.05, **p < 0.01.

other areas of the central nervous system cannot be discounted. RRMS cervical lesions occur preferentially in the dorsal and lateral columns, which include the tracts that serve the dorsal sensory neurons (Eden et al., 2019), a possible explanation for the observation of increased connectivity being detected in the dorsal, but not the ventral network in this cohort. Separating different tracts for DTI measures in healthy and lesioned GM and WM is the next step in untangling the localized effects of tissue damage on connectivity.

Participants differed on the TUG, a sensitive measure of functional mobility, but not on the vibration perception threshold test (although a trend was noted). Those measures characterize a cohort with evident lesional and diffuse pathology, as noted above, who experience minimal clinical symptoms. While no correlations between FC and sensorimotor function were observed, MS participants with an EDSS of 2 (highest in this sample) had high FC values. Inclusion of participants with more severe sensorimotor symptoms would be valuable to investigate the hypothesis that connectivity may be increased as a compensatory mechanism in early-stage MS. Future work will differentiate between ascending and descending WM tracts and examine column-specific DTI measures to further characterize the location and extent of tissue damage in relation to FC. A more thorough assessment of FC and its relation to both microstructural damage and symptoms may help evaluate the presence, amplitude, and time course of compensatory effects, and understand the known discrepancy between radiological disease burden and clinical manifestations.

5. Conclusion

Tissue damage in the CSC was detected with DTI in a cohort of minimally impaired RRMS patients. While FC assessed with rs-fMRI was found to be intact, there was an association between the degree of tissue injury and connectivity strength in the dorsal network. Present findings indicate that the ability to maintain normal FC may be linked with the relative preservation of sensorimotor function in this group in the presence of tissue damage, and provide evidence for the presence of functional compensation mechanisms in the spinal cord.

Declaration of Competing Interest

The authors declare that they have no known competing financial interests or personal relationships that could have appeared to influence the work reported in this paper.

Acknowledgements

The authors thank all study participants and the VUIIS MRI technologists.

Funding

Dr O'Grady was supported by NIH awards KL2TR002245 and K01EB030039. Dr McKnight receives funding from the Radiological Society of North America. Dr Bagnato receives research support from Biogen Idec, the National MS Society (RG-1901-33190), the National Institutes of Health (R21 NS116434-01A1) and the Veterans Health Administration (1T01 CX002160-01A1). This work was supported by grant 1S10OD021771-01 for the 3T MRI, housed in the Vanderbilt Center for Human Imaging, as well as funding from the Conrad Hilton Foundation, National MS Society, and NIH/NINDS 1R01NS109114 and 5R01NS104149.

Appendix A. Supplementary data

Supplementary data to this article can be found online at https://doi.org/10.1016/j.nicl.2022.103127.

References

Agosta, F., Valsasina, P., Caputo, D., Stroman, P.W., Filippi, M., 2008a. Tactile-associated recruitment of the cervical cord is altered in patients with multiple sclerosis. Neuroimage 39, 1542–1548. https://doi.org/10.1016/j.neuroimage.2007.10.048.

Agosta, F., Valsasina, P., Rocca, M.A., Caputo, D., Sala, S., Judica, E., Stroman, P.W., Filippi, M., 2008b. Evidence for enhanced functional activity of cervical cord in relapsing multiple sclerosis. Magn. Reson. Med. 59, 1035–1042. https://doi.org/10.1002/mrm.21595.

Aung, W.Y., Mar, S., Benzinger, T.L., 2013. Diffusion tensor MRI as a biomarker in axonal and myelin damage. Imaging Med. 5, 427–440. https://doi.org/10.2217/iim.13.49.

Baijot, J., Denissen, S., Costers, L., Gielen, J., Cambron, M., D'Haeseleer, M., D'hooghe, M.B., Vanbinst, A.-M., De Mey, J., Nagels, G., Van Schependom, J., 2021. Signal quality as Achilles' heel of graph theory in functional magnetic resonance imaging in multiple sclerosis. Sci. Rep. 11 (1) https://doi.org/10.1038/s41598-021-86792-0.

Barry, R.L., Rogers, B.P., Conrad, B.N., Smith, S.A., Gore, J.C., 2016. Reproducibility of resting state spinal cord networks in healthy volunteers at 7 Tesla. Neuroimage 133, 31–40. https://doi.org/10.1016/j.neuroimage.2016.02.058.

Barry, R.L., Conrad, B.N., Smith, S.A., Gore, J.C., 2018. A practical protocol for measurements of spinal cord functional connectivity. Sci. Rep. 8, 1–10. https://doi.org/10.1038/s41598-018-34841-6.

Basile, B., Castelli, M., Monteleone, F., Nocentini, U., Caltagirone, C., Centonze, D., Cercignani, M., Bozzali, M., 2014. Functional connectivity changes within specific networks parallel the clinical evolution of multiple sclerosis. Mult. Scler. J. 20, 1050–1057. https://doi.org/10.1177/1352458513515082.

Biberacher, V., Boucard, C.C., Schmidt, P., Engl, C., Buck, D., Berthele, A., Hoshi, M.-M., Zimmer, C., Hemmer, B., Mühlau, M., 2015. Atrophy and structural variability of the upper cervical cord in early multiple sclerosis. Mult. Scler. J. 21, 875–884. https://doi.org/10.1177/1352458514546514.

Cader, S., Cifelli, A., Abu-Omar, Y., Palace, J., Matthews, P.M., 2006. Reduced brain functional reserve and altered functional connectivity in patients with multiple sclerosis. Brain 129, 527–537. https://doi.org/10.1093/brain/awh670.

Casserly, C., Seyman, E.E., Alcaide-Leon, P., Guenette, M., Lyons, C., Sankar, S., Svendrovski, A., Baral, S., Oh, J., 2018. Spinal Cord Atrophy in Multiple Sclerosis: A Systematic Review and Meta-Analysis. J. Neuroimaging 28, 556–586. https://doi.org/10.1111/jon.12553.

Chen, Y., Haacke, E.M., Bernitsas, E., 2020. Imaging of the spinal cord in multiple sclerosis: Past, present, future. Brain Sci. 10, 1–19. https://doi.org/10.3390/brainsci10110857.

Ciccarelli, O., Wheeler-Kingshott, C.A., McLean, M.A., Cercignani, M., Wimpey, K., Miller, D.H., Thompson, A.J., 2007. Spinal cord spectroscopy and diffusion-based tractography to assess acute disability in multiple sclerosis. Brain 130, 2220–2231. https://doi.org/10.1093/brain/awm152.

Cohen, Y., Anaby, D., Morozov, D., 2017. Diffusion MRI of the spinal cord: from structural studies to pathology. NMR Biomed. 30 https://doi.org/10.1002/nbm.3592.

Conrad, B.N., Barry, R.L., Rogers, B.P., Maki, S., Mishra, A., Thukral, S., Sriram, S., Bhatia, A., Pawate, S., Gore, J.C., Smith, S.A., 2018. Multiple sclerosis lesions affect intrinsic functional connectivity of the spinal cord. Brain 141, 1650–1664. https://doi.org/10.1093/brain/awy083.

De Leener, B., Lévy, S., Dupont, S.M., Fonov, V.S., Stikov, N., Louis Collins, D., Callot, V., Cohen-Adad, J., 2017. SCT: Spinal Cord Toolbox, an open-source software for processing spinal cord MRI data. Neuroimage 145, 24–43. https://doi.org/10.1016/j.neuroimage.2016.10.009.

Eden, D., Gros, C., Badji, A., Dupont, S.M., De Leener, B., Maranzano, J., Zhuoquiong, R., Liu, Y., Granberg, T., Ouellette, R., Stawiarz, L., Hillert, J., Talbott, J., Bannier, E., Kerbrat, A., Edan, G., Labauge, P., Callot, V., Pelletier, J., Audoin, B., Rasoanandrianina, H., Brisset, J.-C., Valsasina, P., Rocca, M.A., Filippi, M., Bakshi, R., Tauhid, S., Prados, F., Yiannakas, M., Kearney, H., Ciccarelli, O., Smith, S. A., Andrada Treaba, C., Mainero, C., Lefeuvre, J., Reich, D.S., Nair, G., Shepherd, T. M., Charlson, E., Tachibana, Y., Hori, M., Kamiya, K., Chougar, L., Narayanan, S., Cohen-Adad, J., 2019. Spatial distribution of multiple sclerosis lesions in the cervical spinal cord. Brain 142, 633–646. https://doi.org/10.1093/brain/awy352.

Eippert, F., Kong, Y., Winkler, A.M., Andersson, J.L., Finsterbusch, J., Büchel, C., Brooks, J.C.W., Tracey, I., 2017. Investigating resting-state functional connectivity in the cervical spinal cord at 3 T. Neuroimage 147, 589–601. https://doi.org/10.1016/j.neuroimage.2016.12.072.

Faivre, A., Robinet, E., Guye, M., Rousseau, C., Maarouf, A., Le Troter, A., Zaaraoui, W., Rico, A., Crespy, L., Soulier, E., Confort-Gouny, S., Pelletier, J., Achard, S., Ranjeva, J.P., Audoin, B., 2016. Depletion of brain functional connectivity enhancement leads to disability progression in multiple sclerosis: A longitudinal resting-state fMRI study. Mult. Scler. 22, 1695–1708. https://doi.org/10.1177/1352458516628657.

Glover, G.H., Li, T.Q., Ress, D., 2000. Image-based method for retrospective correction of physiological motion effects in fMRI: RETROICOR. Magn. Reson. Med. 44, 162–167. https://doi.org/10.1002/1522-2594(200007)44:1<162::AID-MRM23>3.0.CO;2-E.

Hawellek, D.J., Hipp, J.F., Lewis, C.M., Corbetta, M., Engel, A.K., 2011. Increased functional connectivity indicates the severity of cognitive impairment in multiple sclerosis. Proc. Natl. Acad. Sci. U. S. A. 108, 19066–19071. https://doi.org/10.1073/pnas.1110024108.

Kearney, H., Miller, D.H., Ciccarelli, O., 2015. Spinal cord MRI in multiple sclerosis-diagnostic, prognostic and clinical value. Nat. Rev. Neurol. 11, 327–338. https://doi.org/10.1038/nrneurol.2015.80.

Klawiter, E.C., Schmidt, R.E., Trinkaus, K., Liang, H.F., Budde, M.D., Naismith, R.T., Song, S.K., Cross, A.H., Benzinger, T.L., 2011. Radial diffusivity predicts demyelination in ex vivo multiple sclerosis spinal cords. Neuroimage 55, 1454–1460. https://doi.org/10.1016/j.neuroimage.2011.01.007.

Kong, Y., Eippert, F., Beckmann, C.F., Andersson, J., Finsterbusch, J., Büchel, C., Tracey, I., Brooks, J.C.W., 2014. Intrinsically organized resting state networks in the human spinal cord. Proc. Natl. Acad. Sci. U. S. A. 111, 18067–18072. https://doi.org/10.1073/pnas.1414293111.

Kurtzke, J.F., 1983. Rating neurologic impairment in multiple sclerosis: An expanded disability status scale (EDSS). Neurology 33, 1444–1452. https://doi.org/10.1212/wnl.33.11.1444.

Martin, A.R., Aleksanderek, I., Cohen-Adad, J., Tarmohamed, Z., Tetreault, L., Smith, N., Cadotte, D.W., Crawley, A., Ginsberg, H., Mikulis, D.J., Fehlings, M.G., 2016. Translating state-of-the-art spinal cord MRI techniques to clinical use: A systematic review of clinical studies utilizing DTI, MT, MWF, MRS, and fMRI. NeuroImage Clin. 10, 192–238. https://doi.org/10.1016/j.nicl.2015.11.019.

Mazerolle, E.L., Gawryluk, J.R., Dillen, K.N.H., Patterson, S.A., Feindel, K.W., Beyea, S. D., Stevens, M.T.R., Newman, A.J., Schmidt, M.H., D'Arcy, R.C.N., Yacoub, E., 2013. Sensitivity to White Matter fMRI Activation Increases with Field Strength. PLoS One 8 (3), e58130.

Moll, N.M., Rietsch, A.M., Thomas, S., Ransohoff, A.J., Lee, J.C., Fox, R., Chang, A., Ransohoff, R.M., Fisher, E., 2011. Multiple sclerosis normal-appearing white matter: Pathology-imaging correlations. Ann. Neurol. 70, 764–773. https://doi.org/10.1002/ana.22521.

Naismith, R.T., Xu, J., Klawiter, E.C., Lancia, S., Tutlam, N.T., Wagner, J.M., Qian, P., Trinkaus, K., Song, S.K., Cross, A.H., 2013. Spinal cord tract diffusion tensor imaging reveals Disability substrate in demyelinating disease. Neurology 80, 2201–2209. https://doi.org/10.1212/WNL.0b013e318296e8f1.

Newsome, S.D., Wang, J.I., Kang, J.Y., Calabresi, P.A., Zackowski, K.M., 2011. Quantitative measures detect sensory and motor impairments in multiple sclerosis. J. Neurol. Sci. 305, 103–111. https://doi.org/10.1016/j.jns.2011.03.003.

Nilsagard, Y., Lundholm, C., Gunnarsson, L.G., Dcnison, E., 2007. Clinical relevance using timed walk tests and "timed up and go" testing in persons with multiple sclerosis. Physiother. Res. Int. 12, 105–114. https://doi.org/10.1002/pri.358.

Powers, J., Ioachim, G., Stroman, P., 2018. Ten key insights into the use of spinal cord fmri. Brain Sci. 8 (9), 173.

R Core Team, 2017. R: A language and environment for statistical computing. R Found. Stat. Comput. Vienna, Austria. URL https://www.r-project.org/.

Rocca, M.A., Absinta, M., Valsasina, P., Copetti, M., Caputo, D., Comi, G., Filippi, M., 2012. Abnormal cervical cord function contributes to fatigue in multiple sclerosis. Mult. Scler. J. 18, 1552–1559. https://doi.org/10.1177/1352458512440516.

Rogers, B.P., Gore, J.C., Heo, M., 2008. Empirical comparison of sources of variation for FMRI connectivity analysis. PLoS One 3 (11), e3708.

Sbardella, E., Tona, F., Petsas, N., Pantano, P., 2013. DTI Measurements in Multiple Sclerosis: Evaluation of Brain Damage and Clinical Implications. Mult. Scler. Int. 2013, 1–11. https://doi.org/10.1155/2013/671730.

Smith, S.M., Jenkinson, M., Woolrich, M.W., Beckmann, C.F., Behrens, T.E.J., Johansen-Berg, H., Bannister, P.R., Luca, M.D., Drobnjak, I., Flitney, D.E., Niazy, R.K., Saunders, J., Vickers, J., Zhang, Y., Stefano, N.D., Brady, J.M., Matthews, P.M., De Luca, M., Drobnjak, I., Flitney, D.E., Niazy, R.K., Saunders, J., Vickers, J., Zhang, Y., De Stefano, N., Brady, J.M., Matthews, P.M., 2004. Advances in functional and structural MR image analysis and implementation as FSL. Neuroimage 23 (Suppl 1), S208–S219. https://doi.org/10.1016/j.neuroimage.2004.07.051.

Strik, M., Chard, D.T., Dekker, I., Meijer, K.A., Eijlers, A.J.C., Pardini, M., Uitdehaag, B. M.J., Kolbe, S.C., Geurts, J.J.G., Schoonheim, M.M., 2021. Increased functional sensorimotor network efficiency relates to disability in multiple sclerosis. Mult. Scler. J. 27, 1364–1373. https://doi.org/10.1177/1352458520966292.

Thompson, A.J., Banwell, B.L., Barkhof, F., Carroll, W.M., Coetzee, T., Comi, G., Correale, J., Fazekas, F., Filippi, M., Freedman, M.S., Fujihara, K., Galetta, S.L., Hartung, H.P., Kappos, L., Lublin, F.D., Marrie, R.A., Miller, A.E., Miller, D.H., Montalban, X., Mowry, E.M., Sorensen, P.S., Tintoré, M., Traboulsee, A.L., Trojano, M., Uitdehaag, B.M.J., Vukusic, S., Waubant, E., Weinshenker, B.G., Reingold, S.C., Cohen, J.A., 2018. Diagnosis of multiple sclerosis: 2017 revisions of the McDonald criteria. Lancet Neurol. 17, 162–173. https://doi.org/10.1016/S1474-4422(17)30470-2.

Tommasin, S., De Giglio, L., Ruggieri, S., Petsas, N., Giannì, C., Pozzilli, C., Pantano, P., 2018. Relation between functional connectivity and disability in multiple sclerosis: a non-linear model. J. Neurol. 265, 2881–2892. https://doi.org/10.1007/s00415-018-9075-5.

Valsasina, P., Agosta, F., Absinta, M., Sala, S., Caputo, D., Filippi, M., 2010. Cervical cord functional MRI changes in relapse-onset MS patients. J. Neurol. Neurosurg. Psychiatry 81, 405–408. https://doi.org/10.1136/jnnp.2009.187526.

Valsasina, P., Rocca, M.A., Absinta, M., Agosta, F., Caputo, D., Comi, G., Filippi, M., 2012. Cervical cord FMRI abnormalities differ between the progressive forms of multiple sclerosis. Hum. Brain Mapp. 33, 2072–2080. https://doi.org/10.1002/hbm.21346.

Van Hecke, W., Nagels, G., Emonds, G., Leemans, A., Sijbers, J., Van Goethem, J., Parizel, P.M., 2009. A diffusion tensor imaging group study of the spinal cord in multiple sclerosis patients with and without T2 spinal cord lesions. J. Magn. Reson. Imaging 30, 25–34. https://doi.org/10.1002/jmri.21817.

Vrenken, H., Geurts, J.J.G., Knol, D.L., Polman, C.H., Castelijns, J.A., Pouwels, P.J.W., Barkhof, F., 2006. Normal-appearing white matter changes vary with distance to lesions in multiple sclerosis. Am. J. Neuroradiol. 27, 2005–2011.

Zang, Y.F., Yong, H., Chao-Zhe, Z., Qing-Jiu, C., Man-Qiu, S., Meng, L., Li-Xia, T., Tian-Zi, J., Yu-Feng, W., 2007. Altered baseline brain activity in children with ADHD revealed by resting-state functional MRI. Brain Dev. 29, 83–91. https://doi.org/10.1016/j.braindev.2006.07.002.